

## MORISON FORCING OF COMPLIANT VERTICAL CYLINDERS UNDER THE RELATIVE VELOCITY ASSUMPTION

Nicholas HARITOS

Department of Civil and Agricultural Engineering  
 University of Melbourne, Parkville, VIC 3052  
 AUSTRALIA

### ABSTRACT

This paper presents results from two separate experimental investigations (conducted at the hydraulics laboratory of the National Research Council of Canada in Ottawa and in the Michell laboratory of the University of Melbourne, respectively) of the force characteristics experienced by vertical bottom-mounted cylinders tested for their response to irregular uni-directional Pierson Moskowitz waves. 'Local' values of the Morison force coefficients derived from respective force measurements on a 0.15m and an 0.1m length submerged segment of cylinder under such wave excitation for both rigid and compliant cylinder support conditions are reported for these tests and are found to lend strong evidence for the general acceptance of the 'relative velocity' assumption for the evaluation of hydrodynamic loading on compliant vertical cylinders.

### NOMENCLATURE

$C_A$	added mass coefficient (usually taken as $(C_M - 1)$ )
$C_M$	inertia force coefficient
$C_D$	drag force coefficient under wave excitation
$C'_D$	drag force coefficient derived from 'pluck' tests
$D$	diameter of cylinder
$F_s(t)$	segment force
$f(z,t)$	force per unit length of cylinder
$f$	frequency
$S_*(f)$	spectral density for quantity (*)
$u$	water particle velocity
$\dot{u}$	water particle acceleration
$x$	displacement response
$\dot{x}$	response velocity
$\ddot{x}$	response acceleration
$z$	vertical position from the Mean Water Level
$t$	time
$\eta$	surface elevation profile
$\kappa$	wave number
$\rho$	density of water
$\omega$	circular frequency ( $= 2\pi f$ )

### INTRODUCTION

Morison's equation has been extensively used to predict the in-line hydrodynamic forces experienced by cylindrical elements of an offshore structural form (such as an oil rig) when the cylinder diameter to wavelength ratio,  $(D/\lambda)$ , for the dominant waves responsible for this forcing is outside the diffraction region (diffraction:  $D/\lambda > 0.1$ ) and where 'separation' in the flow around the cylinder can lead to a significant drag force contribution, (Sarpkaya and Isaacson, 1981). In the case of a compliant vertical cylinder, the

'relative flow' assumption for Morison hydrodynamic force leads to a modified version of this equation involving 'relative' velocity and acceleration terms. For the special case of *large* amplitude response of such a cylinder, the so-called 'independent flow fields' assumption has been postulated which in effect considers the cylinder forcing to stem from a 'quasi-rigid cylinder' Morison force equivalent superposed by an additional resistance provided by forcing that would be experienced by such a cylinder in otherwise 'quiescent' flow conditions, (Laya et al, 1984). 'Large' amplitude response, however, is rarely encountered in practice so the 'independent flow fields' approximation should not be generally exercised when modelling for hydrodynamic force on compliant vertical cylinders.

Morison's equation for the force per unit length,  $f(z,t)$ , in the case of a rigid vertical cylinder can be expressed as:

$$f(z,t) = \frac{\pi}{4} \rho D^2 C_M \dot{u}(z,t) + \frac{1}{2} \rho D C_D lu(z,t)u(z,t) \quad (1)$$

where the horizontal water particle velocity and acceleration at level  $z$  from the free surface and at time  $t$  are given by  $u(z,t)$  and  $\dot{u}(z,t)$  respectively and  $C_M$  and  $C_D$  are the inertia and drag force coefficients respectively and  $\rho$  is water density.

$C_M$  and  $C_D$  are often considered to be constants for the cylinder as a whole when applying equation (1) even though they are generally found by researchers working in this field to be both Keulegan Carpenter number (KC) and Reynold's number ( $Re_N$ ) dependent. Consequently some variation of these coefficients with position along the cylinder may reasonably be expected when 'fitting' this equation to experimentally observed force data obtained at local positions along a vertical cylinder. In addition, frequency-dependent versions of these coefficients may alternatively be considered when conducting this 'fitting' using non-linear systems analysis procedures, (Haritos, 1991a).

In the case of a compliant vertical cylinder, where the cylinder response at position  $z$  is given by  $x(z,t)$ , the 'relative flow' assumption for Morison hydrodynamic force leads to a modified version of equation (1) given by

$$f(z,t) = \frac{\pi}{4} \rho D^2 [C_M \dot{u}(z,t) - C_A \ddot{x}(z,t)] + \frac{1}{2} \rho D C_D lu(z,t) - \dot{x}(z,t)(u(z,t) - \dot{x}(z,t)) \quad (2)$$

where  $C_A$ , the added mass coefficient, is often taken to be equivalent to  $(C_M - 1)$ .

The 'independent flow fields' assumption, on the other hand, suggests an interpretation of equation (1) which leads to:

$$f(z,t) = \frac{\pi}{4} \rho D^2 [C_M \dot{u}(z,t) - C_A \ddot{x}(z,t)] + \frac{1}{2} \rho D [C_D lu(z,t)u(z,t) - C'_D |\dot{x}(z,t)|\dot{x}(z,t)] \quad (3)$$

where  $C'_D$  may be different to  $C_D$  as it pertains to the assumption of structure response in quasi-quiescent fluid

conditions, as would be derived from so-called 'pluck' tests.

This paper considers application of the 'relative flow' and 'independent flow fields' assumptions applied to experimental data measurements of the force acting on an instrumented segment of compliant vertical cylinder being subjected to a variety of hydrodynamic inputs which included uni-directional irregular waves conforming to Pierson Moskowitz (PM) wave spectra. Data from both a test program conducted at the hydraulics laboratory of the National Research Council (NRC) of Canada in Ottawa and, separately, from one conducted in the Michell hydraulics laboratory of the University of Melbourne are used in these comparisons.

## SPECTRAL ANALYSIS MODELS

Various modelling strategies for fitting the  $C_M$  and  $C_D$  force coefficients for rigid support conditions and for compliant conditions under (separately) the independent flow fields and relative velocity assumption interpretations of Morison's equation can be adopted from experimentally derived data. In the case of segment force measurements obtained in-line with the direction of wave propagation and uni-directional irregular wave inputs where the wave surface elevation profiles adjacent to the cylinder have also been measured, systems analysis techniques prove to be attractive (Haritos, 1991a). This approach transforms the time series of measurements into the frequency domain and permits both 'constant-valued' and 'frequency-dependent' interpretations for the force coefficients,  $C_M$  and  $C_D$ , to be modelled. Here, a version of the approach that assumes the inertia and drag force contributions to be statistically independent (cross-spectral variations are negligible compared with the individual component spectra), and a constant-valued (frequency-independent) assumption for fitting  $C_M$  and  $C_D$  is adopted.

### Determination of the Water Particle Kinematics

Now, for a time series representation of an irregular wave surface elevation profile,  $\eta(t)$ , taken over  $N$  points  $dt$  apart for a time length of record of  $T$  ( $= Ndt$ ), a Fourier series representation becomes

$$\eta(t) = \sum_{n=1}^{N/2} (a_n \cos \omega_n t + b_n \sin \omega_n t) \quad (4)$$

in which  $(a_n, b_n)$  are the Fourier coefficients for  $\eta(t)$  at a circular frequency  $\omega_n = 2\pi f_n$ , where  $f_n = n/T$  is the frequency in Hertz. The wave number for the  $n^{\text{th}}$  wavelet is given by  $\kappa_n$  and can be obtained from the so-called dispersion relationship from Airy wave theory, viz:

$$\omega_n^2 = g\kappa_n \tanh \kappa_n h \quad (5)$$

Water particle velocity and acceleration at level  $z$  can also be obtained via use of Airy wave theory, so that

$$u(z,t) = \sum_{n=1}^{N/2} \omega_n \frac{\cosh \kappa_n(z+h)}{\sinh \kappa_n h} (a_n \cos \omega_n t + b_n \sin \omega_n t) \quad (6)$$

and

$$\dot{u}(z,t) = \sum_{n=1}^{N/2} \omega_n^2 \frac{\cosh \kappa_n(z+h)}{\sinh \kappa_n h} (b_n \cos \omega_n t - a_n \sin \omega_n t) \quad (7)$$

Equations (6) and (7) allow simulated traces at selected positions  $z$  for the horizontal components of the water particle kinematics to be efficiently generated via Fast Fourier Transform (FFT) algorithms from the Fourier coefficients,  $(a_n, b_n)$ , for any recorded time trace for  $\eta(t)$ .

### Force Spectra for Rigid Support Conditions

In the case of a rigidly supported vertical surface-piercing cylinder, Morison's equation for the force per unit length is given by equation (1) above. The force acting on a segment of length  $\Delta z$  located from position  $z_1$  to  $z_2$  (where  $\Delta z = z_1 - z_2$ ) is therefore given by,  $\hat{F}_s(t)$ , via

$$\begin{aligned} \hat{F}_s(t) &= \int_{z_2}^{z_1} f(z,t) dz \\ &= K_M \int_{z_2}^{z_1} \dot{u}(z,t) dz + K_D \int_{z_2}^{z_1} |u(z,t)|u(z,t) dz \\ &= K_M F_{si}(t) + K_D F_{sd}(t) \end{aligned} \quad (8)$$

where  $K_M = \pi/4 \rho C_M D^2$  and  $K_D = 1/2 \rho C_D D$ , for inertia and drag force contributions,  $F_{si}(t)$  and  $F_{sd}(t)$ , respectively.

Whilst the integral for  $\hat{F}_s(t)$  in equation (8) above (via the  $F_{si}(t)$  and  $F_{sd}(t)$  contributions) can be approximated for a 'small' segment length,  $\Delta z$ , by:

$$\hat{F}_s(t) \approx f\left(\frac{z_1+z_2}{2}, t\right) \Delta z \quad (9)$$

numerical integration is to be preferred for greater accuracy. Considering now the actually recorded time trace for segment force,  $F_s(t)$ , a least squares optimisation procedure on the resultant spectral description, (Haritos and He, 1991), can be adopted for the predicted 'fit' given by  $\hat{F}_s(t)$  via equation (8), viz

$$S_{F_s}(f) \approx S_{\hat{F}_s}(f) = K_M^2 S_{F_{si}}(f) + K_D^2 S_{F_{sd}}(f) \quad (10)$$

to yield 'optimal'  $K_M$  and  $K_D$  from which 'optimal'  $C_M$  and  $C_D$  can then be obtained.

### Force Spectra for Compliant Support Conditions

In the case of a compliant vertical surface-piercing cylinder, equation (2) under the 'relative velocity' assumption for Morison's forcing for  $C_A = C_M - 1$ , leads to:

$$\begin{aligned} \hat{F}_s(t) &= K_1 \int_{z_2}^{z_1} \ddot{x}(z,t) dz = \\ &= K_M \int_{z_2}^{z_1} \dot{u}_r(z,t) dz + K_D \int_{z_2}^{z_1} |u_r(z,t)|u_r(z,t) dz \\ &= K_M F_{sri}(t) + K_D F_{srd}(t) \end{aligned} \quad (11)$$

in which  $u_r$  is the 'relative velocity', given by  $u(z,t) - \dot{x}(z,t)$ ,  $\ddot{u}_r$  is the 'relative acceleration', and  $K_1 = \pi/4 \rho D^2$ .

The terms involving  $\dot{x}(z,t)$  and  $\ddot{x}(z,t)$  in equation (11) need to be determined from the measured trace for response  $x(z_0,t)$  made at level  $z_0$  on the cylinder and from knowledge of its mode shape when undergoing dynamic response. (For the spring end-supported bottom-pivoted conditions pertaining to the compliant cylinders tested in this program, the associated mode shape is a simple straight line). It should also be noted that the time trace for the force measured on the segment concerned needs to be 'corrected' for contributions made to these measurements by the inertia of the segment/force transducer system and for the so called 'P/δ' effects of the gravitational and buoyancy forces acting on it.

A similar spectral 'fitting' procedure to that for the rigid force case, described by equation (10), can then follow from equation (11) to produce 'optimal'  $C_M$  and  $C_D$  that would now apply to compliant cylinder conditions.

## EXPERIMENTAL DETERMINATION OF FORCE COEFFICIENTS: $C_M$ AND $C_D$

The theoretical procedures for fitting 'optimal'  $C_M$  and  $C_D$  via Morison's equation and the interpretations outlined above have been implemented on two separate experimental test programs involving segmented test cylinders and both rigid and compliant support conditions.

### Test Series at the NRC Hydraulics Laboratory

Figure 1 depicts a schematic of the test cylinder used in the NRC experimental program and tested in the 30m x 19.2m multi-directional wave basin testing facility of the hydraulics laboratory. The cylinder is 0.17m in diameter, 2.4m high,

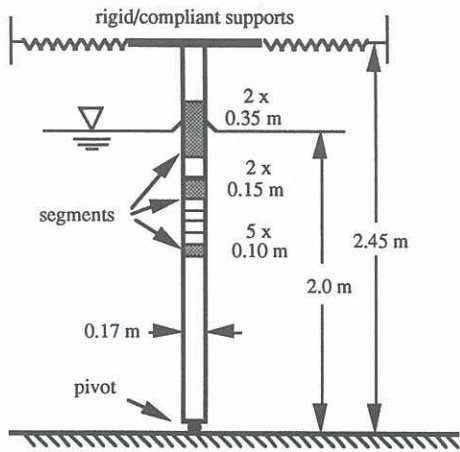


Figure 1 Schematic of Segmented Test Cylinder

with the upper 1.5m divided into nine independent segments, seven of which were completely submerged in the 2m water depth used throughout the test series. Each of the segments was fitted with orthogonally disposed load cells oriented with the in-line and transverse directions (relative to the direction of wave propagation) that measured the segment support force perpendicular to an internal reaction frame onto which they were attached. The cylinder itself was supported by a pinned connection onto the test basin floor and by two pairs of orthogonally disposed springs/rigid links located at its top end and oriented in-line and transverse with the direction of wave propagation. Fixed load cells were attached to the orthogonal spring restraints to provide a measurement of the restraint forces at that level from which the  $(x(t),y(t))$  location of the top of the cylinder under compliant conditions of response could then be inferred. A capacitance wave probe was located at a convenient distance alongside of the cylinder to measure the surface elevation of a range of laboratory generated PM uni-directional waves with frequency at peak wave energy,  $f_p$ , of 0.33, 0.4, 0.5, 0.6 and 0.75 Hz, adopted for these tests.

The PM spectrum is given by

$$S(f) = \frac{0.0005}{f^5} e^{-\left(\frac{f}{4}\right)\left(\frac{f_p}{f}\right)^4} \quad (12)$$

Three different spring sets producing natural frequencies,  $f_0$ , of 0.61, 0.67 and 0.76 Hz were used to provide a range in the condition of compliancy. Data was acquired via a computer based data-acquisition system for 819.2 secs at a rate of 10 Hz for all measurements.

**Results for force coefficients.** Conditions for the rather low KC numbers involved in these tests ( $KC < 5$ ) were observed to be inertia force dominant so that the data series obtained were ill-conditioned for  $C_D$  value determination, (Haritos, 1991b). However, the results for  $C_M$  for both rigid and compliant conditions obtained from this study have indicated a variation with depth in  $C_M$  for this cylinder (see figure 2 for the case of a rigid cylinder with  $f_p = 0.33\text{Hz}$ ) and have inferred values for the cylinder 'as a whole' close to the theoretical 'inertia dominant' value of 2.0 with only a marginal influence (reduction) by degree of compliancy, (see figure 3).

#### Test Series at the Michell Laboratory

The test series at the Michell laboratory was designed to encompass the so-called 'troublesome range' of KC numbers, (viz,  $5 < KC < 15$ ) where both inertia and drag force are important and where drag becomes increasingly significant at higher KC numbers and eventually dominates for  $KC > 15$ .

A single re-locatable segment 0.1m long and instrumented with orthogonally disposed load cells was incorporated into a 0.02m diameter vertical cylinder which was tested in 1m of water and supported in a similar fashion to the NRC test cylinder. The segment was positioned at either

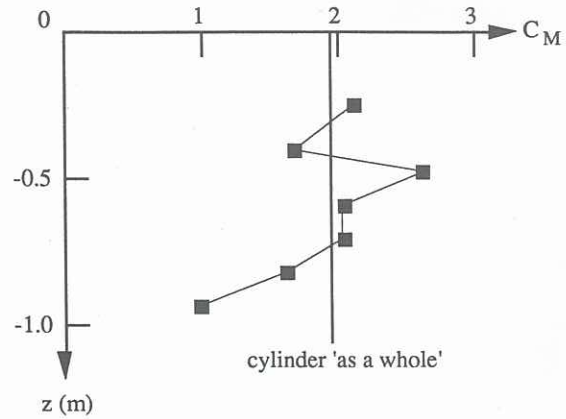


Figure 2  $C_M$  variation with  $z$  via segments ( $f_p=0.33\text{Hz}$ )

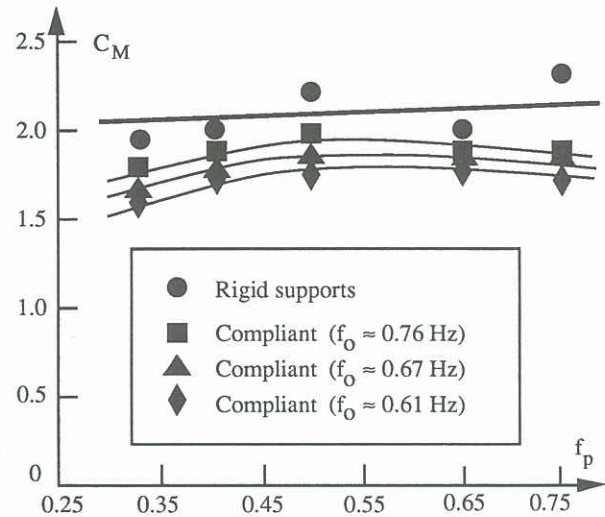


Figure 3 Comparison of  $C_M$  Values with Degree of Compliancy via Segments for Cylinder 'as a Whole'

-0.1 or -0.2m from the MWL and uni-directional PM waves with frequency at peak wave energy,  $f_p$ , of 0.5, 0.6, 0.7 and 0.8 Hz were chosen for this test series. Again, a capacitance wave probe was located alongside the test cylinder to measure the experimentally generated surface elevation profiles. Two spring settings producing structure natural frequencies,  $f_0$ , of 0.7 and 1.0 Hz respectively were adopted for the compliant cylinder conditions. Data was acquired via a micro-computer based data-acquisition system at a rate of 20 Hz for a period of 1000 secs over all measurements.

**Results for force coefficients.** Table I summarises the results for  $C_M/C_D$  fitted to the experimentally recorded segment force data at position  $z = -0.1\text{m}$ , whilst figures 4 and 5 depict the spectral force fits for rigid and compliant support conditions obtained via equations (8) and (11) respectively for the case  $f_p = 0.6\text{Hz}$  for which the inertia and drag force contributions towards the total segment force spectrum were found to be approximately equal (see figure 6). It should be noted that the italicised values for  $C_M$  at KC values of 18 and for  $C_D$  at KC values of 5, although reported in the table, are in fact unreliable since the data is ill-conditioned for estimating inertia force contributions at high KC (drag dominant region) and drag force contributions at low KC (inertia dominant region).

The introduction of compliancy is observed to largely have only a marginal effect on the force coefficients (see Table I). Both force coefficients for the  $f_0 = 0.7\text{ Hz}$  compliant case

TABLE I

Morison Force Coefficients for Rigid and Compliant Supports

Condition	$f_p$ (Hz)	0.5	0.6	0.7	0.8
		KC	18	12	7
Rigid	$C_M$	1.0	1.1	1.3	1.4
	$C_D$	1.7	1.8	1.9	2.2
$f_o = 0.7$ Hz	$C_M$	1.6	1.7	1.6	1.6
	$C_D$	1.8	1.9	2.5	3.0
$f_o = 1.0$ Hz	$C_M$	1.7	1.6	1.6	1.6
	$C_D$	1.5	1.5	1.7	1.9

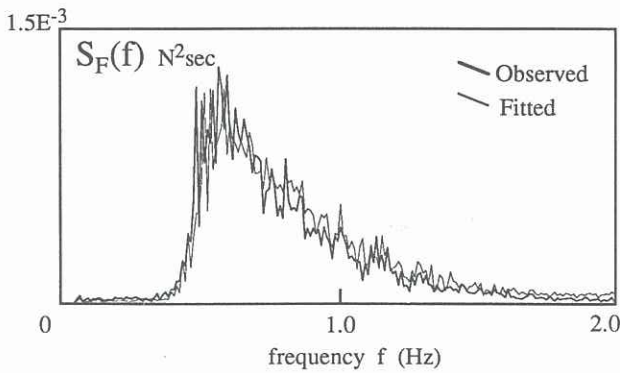


Figure 4 Observed/Fitted Segment Force Spectra, (Rigid)

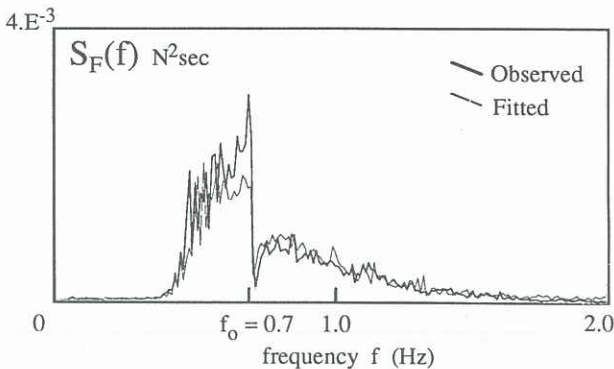


Figure 5 Observed/Fitted Segment Force Spectra, ( $f_o=0.7$ Hz)

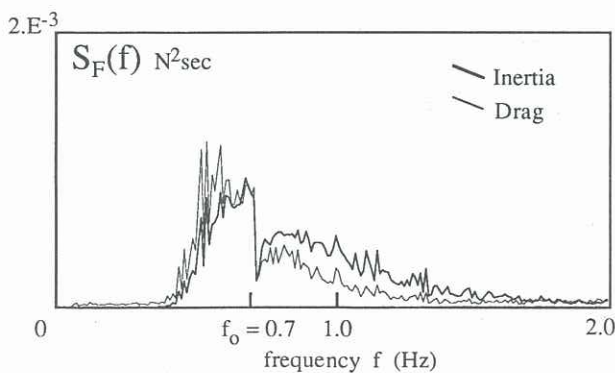


Figure 6 Inertia/Drag Segment Force Spectra, ( $f_o=0.7$ Hz)

are consistently greater than for the rigid case whereas for the case  $f_o = 1.0$  Hz,  $C_M$  values are slightly higher but  $C_D$  values are slightly smaller than for the rigid case. An exception occurs for the case  $f_p = f_o = 0.7$  Hz where the  $C_D$  is substantially higher than for the rigid case. For this case the ratio of standard deviation in cylinder response velocity to water particle velocity at the mid-point of the segment,  $\sigma_x/\sigma_u$ , is approximately 50%, the highest value in the range of PM waves tested, which is largely due to the enhanced 'resonant' response at this frequency as a result of the coincidence of peak wave energy with structure natural frequency. It is clear that application of an 'independent flow fields' assumption (which requires  $\sigma_x/\sigma_u \gg 1$ ) would not be appropriate to the conditions of these tests.

Further, it would appear that the adoption of 'constant-valued' forms (as opposed to 'frequency-dependent' forms) of these force coefficients provide reasonably good spectral fits suggesting that the relative velocity assumption is appropriate to the force modelling being adopted. An interesting feature of figure 5 is the presence of the 'post-resonance dip' at which frequency the relative velocity  $u_r$  is a minimum so that the resultant hydrodynamic force also becomes a minimum - an observation which further supports the contention of the relative velocity assumption in hydrodynamic force modelling.

### CONCLUSIONS

Force coefficients obtained from experimental measurements conducted on instrumented segmented portions of vertical surface-piercing cylinders in both rigid and compliant support states have supported the contention that a 'relative velocity' assumption can be used when applying the Morison hydrodynamic force model.

These force coefficients, derived from two separate test cylinder studies that pertained to inertia dominant conditions ( $KC < 5$ ) and the so-called troublesome KC number range ( $5 < KC < 20$ ) have been found to exhibit a KC dependence and to be only mildly influenced by 'degree of compliancy' (from the rigid to the more flexible conditions of restraint).

Conditions required of the 'independent flow fields' assumption, (viz  $\sigma_x/\sigma_u \gg 1$ ), do not appear to be generally possible for flexible vertical surface-piercing cylinders when subjected to hydrodynamic excitation from irregular unidirectional waves alone so that such an assumption may possibly be limited to structural elements that are very flexible and can exhibit the large amplitude response necessary to this assumption (such as in the case of sub-surface mooring/cable restraint systems).

### ACKNOWLEDGEMENTS

The author would like to acknowledge the assistance of Mr. Ying Qiang He at the University of Melbourne and Mr. Andrew Cornett at the NRC hydraulics laboratory in Ottawa for their respective assistance in the performance of the experimental test programs, the data from which have formed the basis of the paper presented herein. The support of the Australian Research Council via grant No. AA8930685 is also gratefully acknowledged.

### REFERENCES

- HARITOS, N (1991a). Wave force modelling using non-linear systems analysis techniques, Proc 10th Austn Conf on Coastal & Ocean Engineering, Auckland, 289-294.
- HARITOS, N (1991b). The determination of force coefficients from tests on a compliant segmented cylinder, Trans. I.E.Aust., CE33(1), 29-34.
- HARITOS, N AND HE Y Q (1991). Wave force and flow interference on vertical cylinders, Proc. 10th Intl Offshore Mechanics & Arctic Engin. Conf., I(A), 81-86.
- LAYA, E J, CONNOR, J J AND SUNDER, S S (1984) Hydrodynamic forces on flexible offshore structures, ASCE, JI of Engin. Mechs., 110(3), 433-448.
- SARPKAYA, T and ISAACSON, M de St Q (1981) Mechanics of Wave Forces on Offshore Structures, Van Nostrand Reinhold, New York.